

ARTICLE OPEN



Interplay between age, *APOE* ϵ 4 and the metabolome in plasma and brain in Alzheimer's disease

Najaf Amin^{1,13}, Jun Liu^{1,13}, William Sproviero², Matthias Arnold^{3,4,5}, Richa Batra⁶, Bruno Bonnechere^{1,7}, Yu-Jie Chiou^{1,8}, Marco Fernandes², Jan Krumsiek⁶, Danielle Newby², Kwangsik Nho⁹, Jun Pyo Kim⁹, Andrew J. Saykin⁹, Liu Shi^{2,10}, Laura M. Winchester¹⁰, Yang Yang^{1,11}, Alejo J. Nevado-Holgado², Gabi Kastenmüller³, Rima Kaddurah-Daouk^{4,5,12,13} and Cornelia M. van Duijn^{1,13}

© The Author(s) 2025

Age and the ϵ 4 variant of the apolipoprotein E gene (*APOE* ϵ 4) are two major drivers of Alzheimer's disease (AD). *APOE* is also the major determinant of longevity. How age and *APOE* interact in the development of AD is largely unknown. In this study we integrate metabolomics (N = 274,259) and proteomics (N = 54,219) data in plasma from the UK Biobank with the metabolomics (N = 514) and proteomics (N = 618) data in brain from the Religious Orders Study and the Rush Memory and Aging Project (ROSMAP) to understand the interplay of age, *APOE* ϵ 4 and metabolome in the development of AD. We find that levels of β -hydroxybutyrate (BHBA) and branch-chained amino acids (BCAAs) are dysregulated in plasma and brains of AD patients. *APOE* ϵ 4 carriers manifest significantly higher plasma concentration of BHBA that is detectable as early as 37 years of age and remains high throughout the studied age range of 37–73 whereas the plasma concentrations of BCAAs decline in *APOE* ϵ 4 carriers after the age of 58 years. Proteomic signatures of *APOE* ϵ 4, BHBA and BCAAs suggest downregulation of lysosome, immune and insulin-like growth factor (IGF1) transport/uptake pathways in plasma, and downregulation of the tricarboxylic acid (TCA) cycle, neurexins/neuroigins and clathrin-mediated endocytosis pathways in brain. Our data identifies two major shifts in metabolism occurring decades apart over the age course in AD in *APOE* ϵ 4 carriers. These include early ketogenesis that manifests around late 30 s and gluconeogenesis, which manifests around the age of 60 years.

Translational Psychiatry (2025)15:460; <https://doi.org/10.1038/s41398-025-03625-8>

INTRODUCTION

Alzheimer's disease (AD) is characterized by a metabolic shift that occurs in the brain as well as in blood [1]. Metabolomic signatures in the blood involving ketone bodies, branched-chained amino acids (BCAAs), glucose, triglycerides, fatty acids, carnitines, and altered lipid metabolism have been consistently associated to the risk of dementia across studies [2–6]. Blood metabolites may capture the dynamic interplay between the disease processes in and outside the brain and the adaptive mechanisms that occur during the development of dementia and may thus predict the risk and progression of disease [5]. However, beyond prediction, from a biological perspective the relationship between the metabolism in the brain and blood is far from understood. While some of the metabolic changes seen in patients may reflect the disease process, others may be epiphenomena of the complexity of dementia. For example, the 10 years period before the onset of dementia is characterized by anxiety, depression, and weight loss

[7, 8]. The latter is a major determinant of blood metabolite levels and may explain in part the metabolic changes seen in Alzheimer's patients and those with other types of dementia.

The risk for late-onset AD is largely determined by age and the epsilon 4 (ϵ 4) variant of the apolipoprotein E gene (*APOE*) [9]. The effects of age and *APOE* are intertwined, with *APOE* being a major determinant of longevity [10, 11]. Study of aged transgenic *APOE* ϵ 4⁺ mice showed bioenergetic deficits in the brain that involve the TCA cycle at old age [12]. A gap in our knowledge is whether *APOE* is involved in the TCA cycle in humans and how *APOE*'s longitudinal interaction with age influences overall blood metabolic signature. Studies of metabolites influenced by *APOE* over the life course in large population-based studies may help to disentangle the role of *APOE* in aging. Integrating metabolomic and proteomic signatures in blood and brain may shed light on the pathways that can explain the pattern of metabolic changes in future dementia patients.

¹Nuffield Department of Population Health, University of Oxford, Oxford, UK. ²Department of Psychiatry, University of Oxford, Oxford, UK. ³Institute of Computational Biology, Helmholtz Zentrum München, German Research Center for Environmental Health, Neuherberg, Munich, Germany. ⁴Department of Psychiatry and Behavioral Sciences, Duke University, Durham, NC, USA. ⁵Department of Medicine, Duke University, Durham, NC, USA. ⁶Department of Physiology and Biophysics, Institute for Computational Biomedicine, Weill Cornell Medicine, New York, NY, USA. ⁷REVAL Rehabilitation Research Center, Faculty of Rehabilitation Sciences, Hasselt, Belgium. ⁸Department of Psychiatry, Kaohsiung Chang Gung Memorial Hospital, Chang Gung University College of Medicine, Kaohsiung, Taiwan. ⁹Department of Radiology & Imaging Sciences, Center for Neuroimaging, Indiana Alzheimer's Disease Research Center, Indiana University School of Medicine, Indianapolis, IN, USA. ¹⁰Nxera Pharma UK Limited, Cambridge, UK. ¹¹Department of Computer Science and Engineering, Shanghai Jiao Tong University, Shanghai, China. ¹²Duke Institute of Brain Sciences, Duke University, Durham, NC, USA. ¹³These authors contributed equally: Najaf Amin, Jun Liu, Rima Kaddurah-Daouk, Cornelia M. van Duijn. ✉email: rima.kaddurahdaouk@duke.edu; Cornelia.vanDuijn@ndph.ox.ac.uk

Received: 25 September 2024 Revised: 7 August 2025 Accepted: 2 September 2025

Published online: 31 October 2025

In this study, we aim to understand the relationship between metabolic signatures of AD and its early endophenotypes in plasma and brain. To this end, we integrated the data of 274,259 randomly selected participants from the UK Biobank, who were characterised for 172 metabolites assessed by proton nuclear magnetic resonance ($^1\text{H-NMR}$), with that of 516 participants of the Religious Orders Study and the Rush Memory and Aging Project (ROSMAP). We use Mendelian Randomization (MR) to infer whether disease-associated metabolites are a cause or a consequence of the disease process. For the metabolites confirmed with MR, we study the relationship across the *APOE* genotypes over age in plasma in non-demented individuals. To elucidate the molecular mechanisms underlying the metabolic shift observed in AD we identify proteomics pathways involving dysregulation of the metabolites in plasma and brain tissue and compare those to the proteomics pathways disrupted in *APOE* $\epsilon 4$ in plasma and brain.

MATERIAL & METHODS

Study design and participants

We performed a prospective, population-based cohort study based on the UK Biobank dataset [13], which comprised more than 500,000 participants aged from 37 to 73 years at recruitment (2006 to 2010). Among them, a random subset of 274,259 individuals was characterized using the high-throughput $^1\text{H-NMR}$ metabolomics (Nightingale Health, Helsinki, Finland) platform. The participants were registered with the UK National Health Service and from 22 assessment centres across England, Wales, and Scotland using standardized procedures for data collection, which included a wide range of questionnaires, anthropological measurement, clinical biomarkers, genotype data, etc. The imaging data were collected during the third instant follow-up with ~50 K subjects. The participants' hospital inpatient records and death registration were obtained and updated frequently. The updated data until September 2020 were used to define incident diseases in the current study. Further detail on the rationale, study design, survey methods and data collection are available elsewhere [13]. The current study is a part of UK Biobank projects 30418 and 61054.

Brain tissue used in this study was obtained from the autopsy collections of ROSMAP [14], which is a longitudinal cohort study of aging and dementia in elderly nuns, priests, brothers and lay persons. Brain tissue used in this study was obtained from the autopsy collections under brain donation programs with standardized protocol [14, 15]. Tissue was from the dorsolateral prefrontal cortex (Brodmann Area 9 where available). The postmortem neuropathological evaluation, extent of spread of neurofibrillary tangle pathology and neuropathologic diagnoses were made in accordance with established criteria and guidelines [16].

Definitions of dementia and its related endophenotypes

UK Biobank. We defined incident dementia and the major subtypes and onset date based on the previous outcome adjudication guidelines in UK Biobank. In brief, the diseases were based on the primary care or the ICD codes from hospital admission electronic health records in the primary or any secondary causes and/or death register. The earliest recorded code date of diseases was used as the date of disease diagnosis. Prevalent cases were defined as the participants with the disease diagnosis date earlier than the first assessment date, reported in the first time self-reported illness. They were excluded from the analysis. The censor date was defined by either the first recorded date of dementia, death date or the end of the digital recording date, whichever happened first. Two baseline variables of cognitive function were used based on previous publication [17]: (1) fluid intelligence score based on the unweighted sum of the number of correct answers given to the 13 fluid intelligence

questions (field 20016), and (2) reaction time based on mean time to correctly identify matches in the cognitive test (field 20023). The magnetic resonance imaging (MRI) was captured on the median 9.3 years after the collection of the blood samples for the NMR measurements. Four Alzheimer's disease related brain MRI regions (average of left and right sides) were selected, including volumes of the entorhinal cortex (fields 26793 & 26894) and hippocampus (fields 26562 & 26593) from the T1 structural brain MRI, and fractional anisotropy (fields 25494 & 25495) and mean diffusivity (fields 25521 & 25522) in the parahippocampal part of the cingulum from diffusion MRI.

ROSMAP. In ROSMAP, we studied two direct neuropathological variables, including overall amyloid levels and the levels of tangle density, which were measured as the mean of the eight brain regions tested. Three derived neuropathological variables were calculated: global neuropsychiatric scores based on the summary of AD pathology derived from counts of three AD pathologies: neuritic plaques, diffuse plaques, and neurofibrillary tangles; AD diagnosed based on the National Institute on Aging (NIA) Reagan score [18], and neuropsychiatric diagnosis based on Braak and CERAD scores [19]. More details on the study are available on the website of Rush Alzheimer's Disease Center website (RAD; <https://www.radc.rush.edu/>). All subjects gave informed consent.

Covariates used in UK Biobank

The general covariates considered in the analysis included baseline age (field 21022), sex (field 31), body mass index (BMI, field 21001), fasting time (field 74), assessment center (field 54), spectrometer (field 23650), ethnicity (field 21000), smoking status (field 20116), alcohol intake frequency (field 1558), education (field 6138) and medication use (field 20003) from the verbal interview. Medication status was based on the medication codes collected from the verbal interview which were coded to Anatomical Therapeutic Chemical (ATC) codes [20]. The medications considered in the covariates were selected based on our previous publication [21], including five anti-hypertensives (C08, C09, C07, C03 and C02), anti-diabetes (metformin and other anti-diabetics under A10), lipid-lowering drugs (C10), digoxin (C01AA), antithrombotic (B01AC06), proton pump inhibitors (PPI, A02BC), and also 18 drug categories involved in the central nervous system based on 4 digits of the ATC codes.

Genotype measurement in UK Biobank

UK Biobank genotyping was conducted by Affymetrix using a bespoke BiLEVE Axiom array for ~50 K participants and the remaining ~450 K on the Affymetrix UK Biobank Axiom array. As the two arrays are broadly comparable with over 95% overlap in assessed gene variants, they were combined. Genetic data was phased prior to imputation with SHAPEIT3 followed by imputations using IMPUTE2. Details on genetic imputations are provided elsewhere [22]. The *APOE* gene (alleles *APOE* $\epsilon 2$, *APOE* $\epsilon 3$, *APOE* $\epsilon 4$) was directly genotyped and defined by 2 single-nucleotide polymorphisms (SNPs), rs429358 and rs7412. Detailed information on the genotyping process and technical methods are available on the UK Biobank website.

Metabolites and proteomics measurement

UK Biobank. The metabolites in UK Biobank were measured in plasma of ~280,000 participants using targeted high-throughput H-NMR metabolomics platform (Nightingale Health Ltd; biomarker quantification version 2020) [23] which includes 249 metabolite measures simultaneously quantified. They include clinical lipids, lipoprotein subclass profiling with lipid concentrations within 14 subclasses, fatty acid composition, and various low-molecular-weight metabolites such as amino acids, ketone bodies and glycolysis metabolites quantified in molar concentration units. The data obtained from the baseline sampling were used. For the

samples with multiple measurements at baseline, one of the values was extracted at random. A natural logarithm transformation of each metabolite was performed after the zero values were replaced by the lowest value except for zero. In the current study we did not analyse the lipoprotein ratios so in total 172 metabolites were tested for association.

Proteomic profiling of 54,219 participants from the UK Biobank was carried out for protein analytes measured via the Olink Explore platform that links four Olink panels (Cardiometabolic, Inflammation, Neurology, and Oncology). UK Biobank Olink data are provided as Normalized Protein eXpression (NPX) values on a log₂ scale. Details on sample selection, processing, and quality control are provided elsewhere [24].

ROSMAP. Metabolomic data used in the current study was generated in 514 samples with fresh frozen brain tissue - dorsolateral prefrontal cortex (DLPFC) using Metabolon Precision Metabolomics platform which used an ultrahigh performance liquid chromatography-tandem mass spectrometry (UPLC-MS/MS) system (Metabolon, Inc., Morrisville, USA). Details of metabolomic assessments are provided in the supplement and also available in previous publications [25, 26].

The tandem mass tag (TMT) isobaric labelling mass spectrometry method was used to measure the protein abundance from cortical microdissections of the DLPFC of 618 individuals from ROSMAP [27]. Before TMT labelling, individuals were randomized by covariates (such as age, sex, PMI and diagnosis), into batches (eight individuals per batch). MS/MS (MS2) and SPS-MS3 techniques were used for 45 and five TMT batches via the Orbitrap Fusion mass spectrometer (Thermo Fisher Scientific), respectively. The results were normalized and log₂-transformed. Details on sampling, proteomics quantification and quality control are provided in the supplement and elsewhere (<https://www.synapse.org/#!Synapse:syn17015098>).

Statistical analysis

All analyses were performed in R statistical software (version 4.3.1) and the two-tailed test was considered.

Metabolite association analysis. In the UK Biobank, we used a Cox proportional hazards models to estimate the relationship between the metabolite levels at baseline and the risk of incident dementia/AD/VAD during the follow-up. Individuals who were younger than 60 years old at the time of recruitment were excluded from this analysis to make sure cox proportional model's assumptions are not violated. A false discovery rate (FDR) of 0.05 was used to identify significance. For the association analysis, we adjusted for a number of covariates including age, sex, BMI, fasting time, smoking status, alcohol intake frequency, education, ethnicity, physical activity, assessment centre, spectrometer, and 27 drugs which were previously found to be associated with the majority of the Nightingale metabolites [21].

We further tested the association of metabolites with early endophenotypes of AD (fluid intelligence, reaction time, hippocampus volume, entorhinal cortex volume, fractional anisotropy and mean diffusivity in the parahippocampal cingulum). Endophenotypes were modelled as independent variables in a linear regression model adjusted for the same confounders as in the analysis of dementia. Since metabolite spectra may change as a consequence of disease, these analyses were performed in the participants who were free of dementia by the end of the follow-up. Following the protocol from UK Biobank, the head size and all the head position coordinates and imaging site were also adjusted for when analysing brain imaging data.

Mendelian randomization (MR). MR analyses were performed using the 'TwoSampleMR' library of the R software (version 4.3.1). Genetic instruments for AD were extracted from the publicly

available Genome-wide association study (GWAS) of clinically diagnosed AD by Kunkle et al. [28]. The instruments for the metabolites were extracted from the largest GWAS of nightingale metabolites by Richardson et al. [29]. Default settings were used to identify genetic instruments, i.e., $p\text{-value} < 5 \times 10^{-08}$ and $r^2 < 0.001$. Steiger test for directionality was used to elucidate causal direction.

The role of age and APOE on metabolite levels. To determine the impact of age on metabolites (BHBA and BCAAs) across APOE genotypes, we calculated mean levels of metabolites per 6-year age bin across the full age range (37 to 73 years) in non-demented individuals (excluding both prevalent and incident cases of dementia). Difference between means was tested using T-test for the differences of means. A sensitivity analysis was performed in healthy population, excluding all known cases of non-communicable diseases by the end of the follow-up. Further, an age-of-onset association analysis using linear regression analysis adjusted for age at recruitment and sex was performed within APOE ε4 carriers to test if the metabolites were associated with age-of-onset among patients.

Proteomic signatures of APOE, BHBA and BCAAs and pathway analysis

UK Biobank (plasma): Proteomic signatures of APOE, BHBA and BCAAs were constructed in non-demented individuals using a linear regression model adjusting for age, sex and plate. Multiple testing correction was performed using the Benjamini-Hochberg FDR correction. Pathway analysis of significant proteins was performed using the STRINGS database.

ROSMAP (brain): Proteomic signatures were constructed in the brain in all individuals for which there was data on proteomics and metabolomics available (N = 312). Linear regression analysis adjusted for sex was used to perform the association analyses with proteins. Multiple testing correction was performed using the Benjamini-Hochberg FDR correction. Pathway analysis of nominally significant proteins was performed using the STRING database.

RESULTS

Metabolome-wide association of dementia and its endophenotypes

Table 1 summarizes the characteristics of the 119,419 participants included in the metabolome-wide association analysis after exclusions (age <60 years). During follow-up time until June 2023 (mean follow-up years = 12.4), 3344 participants developed dementia, including 1,582 diagnosed with AD and 878 with vascular dementia (VAD). 85 of the 172 metabolites were significantly associated with all-cause dementia (FDR < 0.05) adjusting for ethnicity, age, sex, fasting time, BMI, smoking status, alcohol intake, education, 27 medications for various chronic conditions, assessment centre, fasting time and spectrometer used for the NMR measurements, (Supplementary Table 1). These include increased levels of various large and very large high density lipoprotein (HDL) subfractions, intermediate density lipoproteins (IDLs), sphingomyelins and β-hydroxybutyrate (BHBA, 3-hydroxybutyrate) and decreased levels of various fatty acids, triglycerides, very low density lipoprotein (VLDL) subfractions, and the branched-chain amino acids (BCAAs) valine, leucine, and isoleucine. 77/172 were significantly associated with AD. These included 65 that were significantly associated with dementia and an additional 12 mainly consisting of increased levels of low-density lipoprotein (LDL) subfractions (Supplementary Fig. 1). Association of BHBA was stronger with AD (Beta = 0.16, FDR = 7.2×10^{-04}) compared to all-cause dementia (Beta = 0.098, FDR = 2.1×10^{-03}). VAD showed a slightly different metabolomic

Table 1. Descriptive characteristics of the study population.

Characteristics	Dementia		Alzheimers (AD)		Vascular dementia (VAD)		p-value	
	Total (n = 119419)	No (n = 116011)	Yes (n = 3344)	p-value	No (n = 117826)	Yes (n = 1582)		Yes (n = 878)
Recruitment age, Median (Q1,Q3)	64 (62, 66)	64 (62, 66)	66 (64, 68)	<0.001	64 (62, 66)	66 (64, 68)	66 (64, 68)	<0.001
Sex, n (%)				<0.001				<0.001
Female	62641 (52)	61064 (53)	1547 (46)		61823 (52)	805 (51)	344 (39)	
Male	56778 (48)	54947 (47)	1797 (54)		56003 (48)	777 (49)	534 (61)	
Smoking status, n (%)				<0.001				<0.001
Never	59042 (50)	57505 (50)	1505 (45)		58290 (50)	747 (48)	369 (42)	
Previous	49923 (42)	48384 (42)	1511 (46)		49222 (42)	698 (45)	411 (47)	
Current	9757 (8)	9462 (8)	292 (9)		9638 (8)	118 (8)	89 (10)	
Alcohol_freq, n (%)				<0.001				<0.001
Never	10115 (8)	9632 (8)	472 (14)		9904 (8)	211 (13)	127 (14)	
Special occasions only	14441 (12)	13947 (12)	485 (15)		14213 (12)	224 (14)	119 (14)	
One to three times a month	11932 (10)	11589 (10)	333 (10)		11781 (10)	149 (9)	86 (10)	
Once or twice a week	28784 (24)	28026 (24)	747 (22)		28379 (24)	400 (25)	205 (23)	
Three or four times a week	26405 (22)	25767 (22)	632 (19)		26109 (22)	296 (19)	162 (18)	
Daily or almost daily	27544 (23)	26864 (23)	664 (20)		27248 (23)	297 (19)	178 (20)	
Body mass index, Median (Q1,Q3)	27.02 (24.52, 29.99)	27.02 (24.52, 29.98)	27.18 (24.52, 30.39)	0.101	27.02 (24.52, 30)	26.94 (24.28, 29.86)	27.8 (25.15, 31.24)	<0.001
Physical activity (IPAQ), n (%)				<0.001				<0.001
low	16221 (17)	15700 (17)	506 (20)		16024 (17)	196 (17)	154 (23)	
moderate	39043 (42)	38004 (42)	1025 (41)		38560 (42)	478 (40)	255 (38)	
high	38691 (41)	37706 (41)	971 (39)		38181 (41)	508 (43)	257 (39)	
Ethnicity, n (%)				<0.001				<0.001
British	110109 (93)	107014 (93)	3035 (91)		108656 (93)	1444 (92)	797 (91)	
White	129 (0)	120 (0)	9 (0)		122 (0)	6 (0)	2 (0)	
Mixed	12 (0)	11 (0)	1 (0)		11 (0)	1 (0)	0 (0)	
Asian or Asian British	5 (0)	5 (0)	0 (0)		5 (0)	0 (0)	0 (0)	
Black or Black British	4 (0)	3 (0)	1 (0)		4 (0)	0 (0)	1 (0)	
Chinese	145 (0)	145 (0)	0 (0)		145 (0)	0 (0)	0 (0)	
Other ethnic group	500 (0)	489 (0)	11 (0)		496 (0)	4 (0)	4 (0)	
Irish	2871 (2)	2754 (2)	116 (3)		2827 (2)	44 (3)	37 (4)	
Any other white background	2746 (2)	2685 (2)	61 (2)		2718 (2)	28 (2)	17 (2)	
White and Black Caribbean	47 (0)	43 (0)	4 (0)		45 (0)	2 (0)	1 (0)	
White and Black African	91 (0)	90 (0)	1 (0)		91 (0)	0 (0)	0 (0)	
White and Asian	127 (0)	123 (0)	4 (0)		123 (0)	4 (0)	0 (0)	
Any other mixed background	854 (1)	830 (1)	24 (1)		845 (1)	9 (1)	4 (0)	
Indian	178 (0)	173 (0)	5 (0)		175 (0)	3 (0)	0 (0)	
Pakistani	14 (0)	14 (0)	0 (0)		14 (0)	0 (0)	0 (0)	
Bangladeshi	220 (0)	214 (0)	6 (0)		216 (0)	4 (0)	0 (0)	
Any other Asian background	502 (0)	469 (0)	33 (1)		483 (0)	19 (1)	5 (1)	
Caribbean	288 (0)	278 (0)	10 (0)		284 (0)	4 (0)	7 (1)	
African	7 (0)	6 (0)	1 (0)		7 (0)	0 (0)	1 (0)	
Any other Black background								

Table 1. continued

Characteristics	Dementia		Alzheimers (AD)		Vascular dementia (VAD)		p-value			
	Total (n = 119419)	No (n = 116011)	Yes (n = 3344)	p-value	No (n = 117826)	Yes (n = 1582)		p-value		
Volume hippocampus (Left), Median (Q1,Q3)	3762.9 (3520.5, 4034.07)	3763.9 (3522.98, 4034.65)	3476.8 (3283.5, 3704.9)	<0.001	3763.3 (3522.5, 4034.4)	3476.8 (3262.7, 3583.8)	<0.001	3763.3 (3521.2, 4034.3)	3476.8 (3425.3, 3654.2)	0.009
Volume hippocampus (Right), Median (Q1,Q3)	3927.25 (3666.62, 4205.65)	3928.15 (3668.85, 4205.98)	3568.7 (3328.65, 3860.2)	<0.001	3927.7 (3667.9, 4205.8)	3463.7 (3229.9, 3810.8)	<0.001	3927.6 (3667.2, 4205.8)	3657.6 (3337.2, 3796.5)	0.008
Volume entorhinal cortex (Right), Median (Q1,Q3)	1789 (1561, 2051)	1789.5 (1561, 2052)	1641 (1403, 1842)	0.005	1789 (1561, 2052)	1543 (1369, 1815)	0.061	1789 (1561, 2052)	1603 (1439, 1722)	0.019
Volume entorhinal cortex (Left), Median (Q1,Q3)	1911.5 (1661, 2186.75)	1912 (1661.25, 2187)	1685 (1493, 2078)	0.023	1912 (1661, 2187)	1836 (1478, 2067)	0.195	1912 (1661, 2187)	1634 (1488, 1834)	0.028
Headsize, Median (Q1,Q3)	1.28 (1.2, 1.37)	1.28 (1.2, 1.37)	1.31 (1.21, 1.39)	0.408	1.28 (1.2, 1.37)	1.32 (1.21, 1.38)	0.392	1.28 (1.2, 1.37)	1.33 (1.32, 1.4)	0.089
Fractional anisotropy (Right), Median (Q1,Q3)	0.46 (0.43, 0.48)	0.46 (0.43, 0.48)	0.45 (0.42, 0.46)	0.027	0.46 (0.43, 0.48)	0.42 (0.4, 0.44)	0.002	0.46 (0.43, 0.48)	0.48 (0.45, 0.48)	0.387
Fractional anisotropy (Left), Median (Q1,Q3)	0.46 (0.43, 0.48)	0.46 (0.43, 0.48)	0.44 (0.43, 0.47)	0.096	0.46 (0.43, 0.48)	0.42 (0.41, 0.44)	0.002	0.46 (0.43, 0.48)	0.47 (0.46, 0.47)	0.372
Mean diffusivity (Right), Median (Q1,Q3)	0.000762(0.000738, 0.000787)	0.000762(0.000738, 0.000787)	0.000781 (0.000741, 0.00082)	0.048	0.000762(0.000738, 0.000787)	0.000723 (0.000721, 0.000768)	0.13	0.000765(0.000742, 0.000789)	0.000772, (0.000771)	0.247
Mean diffusivity (Left), Median (Q1,Q3)	0.000765(0.000742, 0.000789)	0.000765 (0.000742, 0.000787)	0.000781(0.000746, 0.00082)	0.036	0.000765 (0.000742, 0.000789)	0.000814(0.000803, 0.000818)	<0.001	0.000765(0.000742, 0.000789)	0.000772, (0.000771)	<0.001
Reaction time, Median (Q1,Q3)	567 (508, 645)	567 (508, 645)	597 (528, 687)	<0.001	567 (508, 645)	590 (527, 680)	<0.001	567 (508, 645)	613 (539, 695)	<0.001
Fluid intelligence, Median (Q1,Q3)	6 (4, 7)	6 (4, 7)	5 (4, 7)	<0.001	6 (4, 7)	5 (4, 6)	<0.001	6 (4, 7)	5 (3, 6)	<0.001
Handgrip strength (Left), Median (Q1,Q3)	26 (20, 36)	26 (20, 36)	26 (18, 34)	<0.001	26 (20, 36)	25 (18, 34)	<0.001	26 (20, 36)	28 (20, 36)	0.859
Handgrip strength (Right), Median (Q1,Q3)	28 (22, 38)	28 (22, 38)	28 (21, 37)	<0.001	28 (22, 38)	28 (20, 36)	<0.001	28 (22, 38)	30 (22, 38)	0.886
AD_time, Median (Q1,Q3)	4538 (4229, 4812)	4546 (4241, 4816)	4122 (3308.25, 4583)	<0.001	4544 (4237, 4815)	3621 (2838.5, 4167)	<0.001	4539 (4230, 4812)	4237 (3500.5, 4670)	<0.001
dementia_time, Median (Q1,Q3)	4531 (4224, 4810)	4546 (4242, 4816)	3608.5 (2854, 4196)	<0.001	4539 (4230, 4812)	3617 (2858, 4215.5)	<0.001	4537 (4228, 4812)	3491 (2749, 4128)	<0.001
VAD_time, Median (Q1,Q3)	4541 (4231, 4814)	4546 (4242, 4816)	4260 (3518, 4678)	<0.001	4543 (4235, 4814.5)	4355.5 (3741.75, 4726.25)	<0.001	4544 (4236, 4815)	3640.5 (2926.75, 4228.5)	<0.001
Fasting time (hrs), Median (Q1,Q3)	3 (3, 4)	3 (3, 4)	4 (3, 5)	<0.001	3 (3, 4)	4 (3, 5)	<0.001	3 (3, 4)	4 (3, 5)	<0.001
Medication use										
Antidiabetics (A10), n (%)	113349 (95)	110334 (95)	2964 (89)	<0.001	111911 (95)	1425 (90)	<0.001	112609 (95)	740 (84)	<0.001
Yes	6070 (5)	5677 (5)	380 (11)	<0.001	5915 (5)	157 (10)	0.047	5932 (5)	138 (16)	<0.001
Antihypertensives (C02), n (%)	116582 (98)	113313 (98)	3207 (96)	<0.001	115040 (98)	1532 (97)		115746 (98)	836 (95)	<0.001
Yes	2837 (2)	2698 (2)	137 (4)	<0.001	2786 (2)	50 (3)	0.156	2795 (2)	42 (5)	<0.001
Diuretics (C03), n (%)										

Table 1. continued

Characteristics	Dementia		p-value	Alzheimers (AD)		p-value	Vascular dementia (VAD)		p-value
	Total (n = 119419)	No (n = 116011)		Yes (n = 3344)	No (n = 117826)		Yes (n = 1582)	No (n = 118541)	
No	104407 (87)	101535 (88)	2820 (84)	103031 (87)	1364 (86)	103704 (87)	703 (80)		
Yes	15012 (13)	14476 (12)	524 (16)	14795 (13)	218 (14)	14837 (13)	175 (20)	<0.001	
Beta blocking agents (C07), n (%)									
No	106139 (89)	103304 (89)	2780 (83)	104777 (89)	1355 (86)	105456 (89)	683 (78)		
Yes	13280 (11)	12707 (11)	564 (17)	13049 (11)	227 (14)	13085 (11)	195 (22)	0.002	
Calcium channel blockers (C08), n (%)									
No	105519 (88)	102679 (89)	2790 (83)	104144 (88)	1358 (86)	104831 (88)	688 (78)		
Yes	13900 (12)	13332 (11)	554 (17)	13682 (12)	224 (14)	13710 (12)	190 (22)	<0.001	
Renin-angiotensin system drugs (C09), n (%)									
No	94239 (79)	91844 (79)	2352 (70)	93053 (79)	1177 (74)	93700 (79)	539 (61)		
Yes	25180 (21)	24167 (21)	992 (30)	24773 (21)	405 (26)	24841 (21)	339 (39)	<0.001	
Lipid lowering (C10), n (%)									
No	81670 (68)	79753 (69)	1886 (56)	80716 (69)	944 (60)	81258 (69)	412 (47)		
Yes	37749 (32)	36258 (31)	1458 (44)	37110 (31)	638 (40)	37283 (31)	466 (53)	<0.001	
Opioids (N02A), n (%)									
No	111323 (93)	108324 (93)	2946 (88)	109901 (93)	1414 (89)	110564 (93)	759 (86)		
Yes	8096 (7)	7687 (7)	398 (12)	7925 (7)	168 (11)	7977 (7)	119 (14)	<0.001	
Analgesics & antipyretics (N02B), n (%)									
No	77513 (65)	75708 (65)	1773 (53)	76612 (65)	891 (56)	77114 (65)	399 (45)		
Yes	41906 (35)	40303 (35)	1571 (47)	41214 (35)	691 (44)	41427 (35)	479 (55)	0.104	
Antimigraine (N02C), n (%)									
No	118218 (99)	114833 (99)	3321 (99)	116634 (99)	1573 (99)	117348 (99)	870 (99)		
Yes	1201 (1)	1178 (1)	23 (1)	1192 (1)	9 (1)	1193 (1)	8 (1)	<0.001	
Antiepileptics (N03A), n (%)									
No	117262 (98)	114005 (98)	3199 (96)	115727 (98)	1527 (97)	116437 (98)	825 (94)		
Yes	2157 (2)	2006 (2)	145 (4)	2099 (2)	55 (3)	2104 (2)	53 (6)	0.025	
Anticholinergics (N04A), n (%)									
No	119337 (100)	115940 (100)	3335 (100)	117747 (100)	1578 (100)	118460 (100)	877 (100)		
Yes	82 (0)	71 (0)	9 (0)	79 (0)	4 (0)	81 (0)	1 (0)	<0.001	
Dopaminergic (N04B), n (%)									
No	118965 (100)	115672 (100)	3235 (97)	117393 (100)	1561 (99)	118094 (100)	871 (99)		
Yes	454 (0)	339 (0)	109 (3)	433 (0)	21 (1)	447 (0)	7 (1)	0.077	
Antipsychotics (N05A), n (%)									
No	118488 (99)	115138 (99)	3292 (98)	116913 (99)	1563 (99)	117626 (99)	862 (98)		
Yes	931 (1)	873 (1)	52 (2)	913 (1)	19 (1)	915 (1)	16 (2)	0.005	
Anxiolytics (N05B), n (%)									
No	118883 (100)	115508 (100)	3314 (99)	117304 (100)	1567 (99)	118012 (100)	871 (99)		
Yes	536 (0)	503 (0)	30 (1)	522 (0)	15 (1)	529 (0)	7 (1)	0.181	
Hypnotics & sedatives (N05C), n (%)									
No	118327 (99)	114978 (99)	3289 (98)	116754 (99)	1562 (99)	117466 (99)	861 (98)		
Yes	1092 (1)	1033 (1)	55 (2)	1072 (1)	20 (1)	1075 (1)	17 (2)	<0.001	

signature associating with only 36/172 metabolites, of which 16 overlapped with dementia and AD (Supplementary Table 1, Supplementary Fig. 1). Figure 1 shows that all-cause dementia and AD strongly cluster while VAD clusters more weakly, failing to associate to the BCAAs leucine and isoleucine, BHBA, HDL levels, triglyceride and phospholipid levels in various lipid particles and most VLDL particles. VAD appears to be unique associated to high levels of apolipoprotein B, (large) LDL concentration, phospholipids in very large high-density lipoprotein (HDL), and total, remnant and free cholesterol and low albumin levels. Sensitivity analysis (performed for AD) by additionally removing all prevalent and incident cases of CVD, diabetes, and kidney and liver diseases did not influence the results (Supplementary Table 2, Supplementary Fig. 2).

When comparing the metabolomic signatures of dementia with that of its early endophenotypes including volumes of hippocampus and entorhinal cortex, fractional anisotropy (FA) and mean diffusivity (MD) in parahippocampal cingulum, fluid intelligence and reaction time in dementia-free individuals, results were overall consistent for VLDL subfractions, triglycerides, BCAAs and fatty acids (Fig. 1). Also consistent with the findings for dementia, high levels of BHBA were significantly associated with lower fluid intelligence (Beta = -0.06 , FDR = 1.6×10^{-10} , Supplementary Table 3) and increased reaction time (Beta = 1.26 , FDR = 2.4×10^{-05}). For HDL, LDL and IDL subfractions results were inconsistent between dementia and its early endophenotypes in direction of the effect estimates (Fig. 1). Taken together, our findings suggest that the metabolic shift occurs several years prior to the diagnosis of dementia. However, as the disease process is insidious in the prodromal stage for most dementias, we cannot exclude that the metabolic shift is a consequence of an early phase of the disease.

Inferring causal direction with Mendelian Randomisation (MR)

We used MR to infer whether the metabolic shift we observed is upstream or downstream of the disease process. MR was only possible for AD, which is well characterized genetically. At present, data on genetics of VAD does not allow a reliable MR. Results of MR for AD suggest that changes in metabolite levels of BHBA and BCAAs (valine, leucine and isoleucine) (Supplementary Table 4) are downstream of the disease process. Other metabolites that showed significance in MR were inconsistent in the effect direction with the association results and hence were excluded from further analyses. There was no significant evidence for any of the metabolites that they are causally associated to AD. The sensitivity analysis shows that the results for BHBA are only driven by the *APOE* locus (rs429358/rs7412) (Supplementary Fig. 3), which is the key instrumental variable for both AD and BHBA. However, the test for horizontal pleiotropy was not significant (Supplementary Table 5) and the Steiger test for directionality suggests that high plasma concentration of BHBA is a consequence of the disease process (Supplementary Table 6).

The interplay between *APOE*, age, BHBA and BCAAs

To further investigate the relationship of BHBA and BCAAs in plasma with *APOE* over the lifetime, we determined the mean concentrations of these metabolites across *APOE* genotypes and age groups in the UK Biobank population who did not develop dementia during follow-up ($n = 268,368$; age ranging from 37 to 73 years, Fig. 2). Plasma levels of BHBA increase with age across all the *APOE* genotypes (Fig. 2). However, BHBA levels in the *APOE* $\epsilon 44$ and $\epsilon 24/\epsilon 34$ carriers were significantly higher compared to the non-carriers across all age groups (Fig. 2, Supplementary Table 7). Since *APOE* is a pleiotropic gene with effects on several other diseases that occur in midlife, early differences in the concentration of BHBA across different *APOE* genotypes may also be attributed to these midlife diseases. However, a sensitivity analysis excluding all incident and prevalent cases of non-communicable

diseases showed the same pattern for BHBA (Supplementary Fig. 4) and the differences in BHBA concentration across the *APOE* genotypes remain significant. Taking together this finding with that of the MR suggests that high plasma levels of BHBA may be an early marker of AD and detectable as early as in the late 30 s.

For BCAAs (valine, leucine and isoleucine), their levels increase until age 58 and do not significantly differ across the age groups between the carriers and non-carriers of the *APOE* $\epsilon 4$ allele (Fig. 2, Supplementary Table 8). Of note for BCAAs is that after an age of 60, a sharp (significant) decline in *APOE* $\epsilon 44$ carriers is observed (Fig. 2), suggesting that BCAAs change as part of the aging process. Combining the trends over age and by *APOE* genotypes with the results of MR suggest that changes in BCAAs are most likely a later consequence of dementia than the changes in BHBA. In line with these findings, increase in the levels of BHBA was significantly associated with lower age-of-onset ($\beta = -2.48$, p -value = 3.6×10^{-03}) and higher levels of valine ($\beta = 6.09$, p -value = 9.3×10^{-07}), leucine ($\beta = 8.61$, p -value = 4.9×10^{-06}) and isoleucine ($\beta = 11.77$, p -value = 6.7×10^{-05}) were associated with higher age-of-onset among *APOE* $\epsilon 4$ carriers.

Comparing proteomic signatures of *APOE* $\epsilon 4$, BHBA and BCAAs in plasma

To understand the interplay between the *APOE* gene, BHBA and BCAAs in plasma, we identified proteomic signatures of *APOE* $\epsilon 4$ and compared these with the proteomic signatures of BHBA and BCAAs in non-demented individuals in the UK Biobank. There were 257/2923 proteins significantly associated (FDR < 0.05) with *APOE* $\epsilon 4$, of which 180 were downregulated and 77 were upregulated (Supplementary Table 9). The downregulated proteins were enriched in pathways involved in the regulation of insulin-like growth factor (IGF) transport and uptake (Reactome; FDR < 4.9×10^{-09}), immune system (Reactome; FDR < 1.5×10^{-08}), and lysosome (KEGG; FDR = 2.9×10^{-13}) among several others that were less significant (Supplementary Table 10). Of these, IGF transport/uptake and the immune system were also involved in the upregulation of plasma BHBA and downregulation of BCAAs (Supplementary Tables 11 and 12, Supplementary Figs. 5 and 6), with immune system (FDR = 5.2×10^{-64}), more specifically involving neutrophil degranulation (6.6×10^{-24}) being much more significant in the upregulation of the plasma levels of BHBA. Further, upregulated BHBA associated proteins in plasma were also significantly enriched in the lysosome pathway (KEGG; FDR = 1.4×10^{-07}) (Supplementary Fig. 6). Looking into the cellular localization, the *APOE* $\epsilon 4$ -downregulated proteins were enriched in extracellular region (FDR = 2.1×10^{-41}), lysosome (FDR = 7.9×10^{-18}) and azurophil granules (FDR = 4.8×10^{-09}) (Supplementary Fig. 7). All three cell components were also significantly enriched with proteins that were associated with increased levels of BHBA in plasma, while the proteins associated with low concentration of BCAAs were enriched in extracellular region, vesicle, cell surface and plasma membrane.

Proteins that were upregulated in *APOE* $\epsilon 4$ carriers in plasma were not enriched in any specific pathway (Supplementary Table 13). Proteins that were downregulated with increased plasma BHBA concentration were involved in glycosaminoglycan binding, heparin binding, vitamin digestion and absorption, nitrogen metabolism and neurogenesis among several other pathways (Supplementary Table 14). Proteins that were upregulated with high levels of BCAAs (valine) were enriched in pathways involved in the immune system, platelet activation, apoptosis and lysosome among several others (Supplementary Table 15).

The two known proteomic markers of AD, i.e., neurofilament light (NEFL) and glial fibrillary acidic protein (GFAP) were significantly associated with BHBA (NEFL; $\beta = 0.05$, FDR = 6.1×10^{-07} , GFAP; $\beta = 0.086$, FDR = 2.5×10^{-19}), valine (NEFL; $\beta = -0.04$, FDR = 7.2×10^{-50} , GFAP; $\beta = -0.04$, FDR = 1.0×10^{-58}), leucine (NEFL; $\beta = -0.05$, FDR = 2.8×10^{-46} , GFAP;

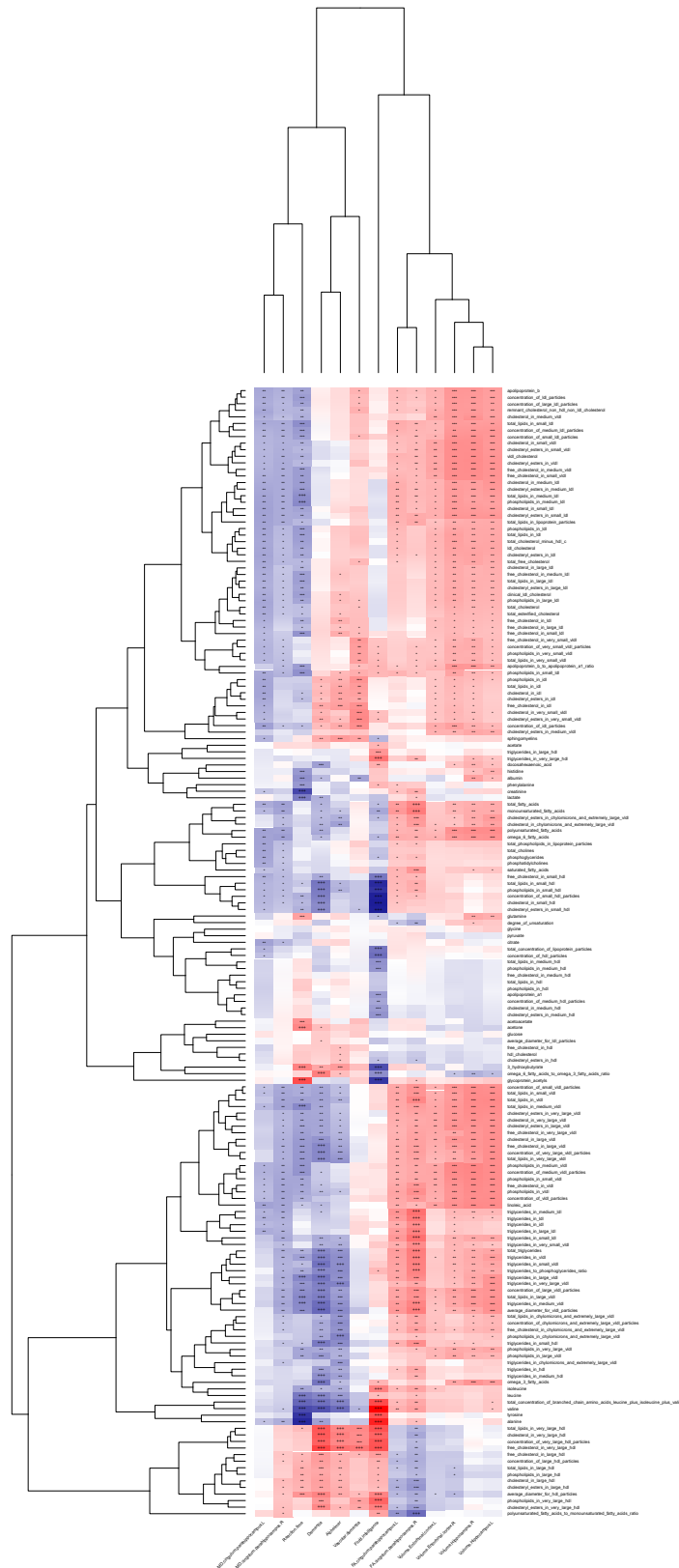


Fig. 1 Heatmap illustrating the results of metabolome-wide association analysis. Z-scores from the association analyses are plotted. Red colour indicates positive association and blue indicates negative association. Significant associations are marked as 0.01 < FDR < 0.05 (*), 0.001 < FDR < 0.01 (**), 0.0001 < FDR < 0.001 (***) and FDR < 0.0001 (+++). MD mean diffusivity, FA fractional anisotropy.

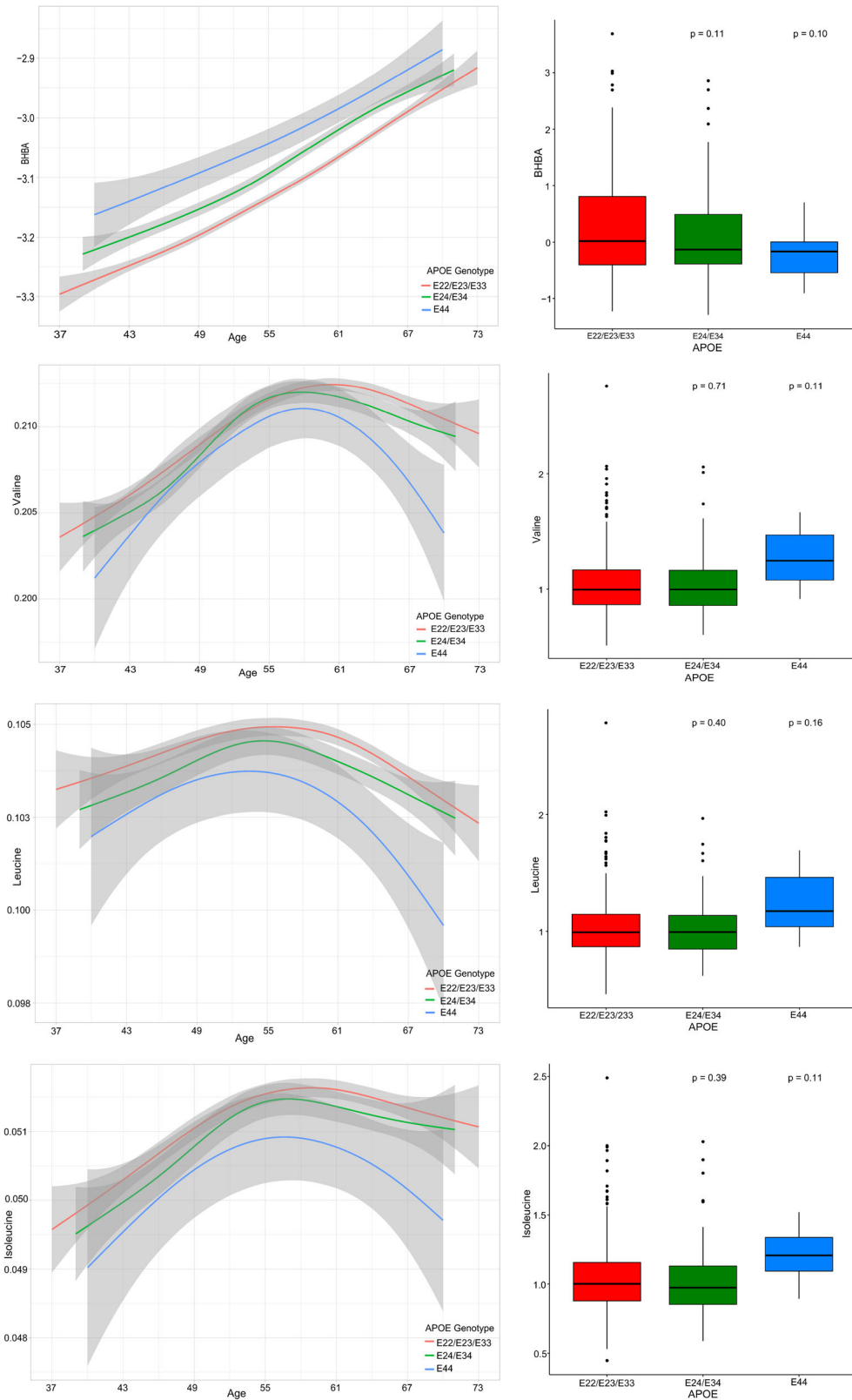


Fig. 2 Levels of β -Hydroxybutyrate (BHBA) and branch chain amino acids (BCAAs) across APOE genotypes in plasma and brain. Blood (UKBB) and brain (ROSMAP) levels of identified metabolites by APOE genotype levels. Left panels show the levels of BHBA and BCAAs over age by APOE genotypes in blood in the UK Biobank. Right panels show the distribution of BHBA and BCAAs by APOE genotypes in the brain in the ROSMAP cohort.

beta = -0.05, FDR = 1.2×10^{-73}) and isoleucine (NEFL; beta = -0.04, FDR = 7.3×10^{-21} , GFAP; beta = -0.07, FDR = 1.5×10^{-65}) (Supplementary Table 9). These findings are consistent with their association with AD.

APOE ϵ 4, BHBA and BCAAs and AD related pathology in the brain

We next studied association of BCAAs and BHBA with AD and AD pathology in the brain tissue from the ROSMAP study. In the brain, high valine levels were significantly associated with varying AD-related pathological changes, including tau pathology as measured with the Braak stage (beta = 0.60, $p = 2.9 \times 10^{-3}$), neuritic plaques based on the Consortium to Establish a Registry for Alzheimer's Disease (CERAD) score (beta = 0.79, $p = 2.0 \times 10^{-05}$), and AD, (beta = 1.44, $p = 9.1 \times 10^{-04}$). Other BCAAs (leucine and isoleucine) showed a similar pattern of association. Low levels of BHBA were significantly associated with Braak stage (beta = -0.05, $p = 7.3 \times 10^{-03}$) but not with amyloid pathology (Supplementary Table 16). When stratified by the APOE genotypes, APOE ϵ 44 exhibit lower levels (albeit not significant) of BHBA and higher levels of BCAAs compared to non-carriers and heterozygous carriers (Fig. 2), which is in the opposite direction compared to the observations in the plasma.

Proteomic signatures of APOE, BHBA and BCAAs in the brain

To understand the interplay between the APOE gene, BHBA and BCAAs in the brain, we first identified the proteomic signatures of APOE, BHBA and BCAA in the brain. Using the proteomic signatures, we then identified molecular pathways involved in up-/downregulation of these metabolites in the brain and compared those with the pathways differentially regulated in APOE ϵ 4 carriers (Supplementary Table 17). Proteins that were downregulated in the APOE ϵ 4 carriers in the brain tissue were enriched in pathways including neurexins & neuroligins (Reactome; FDR = 2.4×10^{-09}), TCA cycle (Reactome; FDR < 3.6×10^{-07}) and clathrin-mediated endocytosis (Reactome; FDR = 2.3×10^{-04}) (Supplementary Table 18).

Proteins that were upregulated with high levels of BHBA in the brain were significantly enriched in the mitochondrial translation pathways (Reactome; FDR < 7.81×10^{-10} ; Supplementary Table 19), while those involved in downregulation were enriched in cholesterol metabolism (Reactome; FDR = 2.9×10^{-04}) and immune system (Reactome; FDR = 2.1×10^{-03} ; Supplementary Table 20). Proteins that were upregulated with higher levels of BCAA (valine) were enriched in immune system regulation (Reactome; FDR = 1.8×10^{-14} ; Supplementary Table 21) and those downregulated were enriched in the processing of mRNA (Reactome; FDR = 2.5×10^{-07}) and neurexin & neuroligins/synapse formation (Reactome; FDR = 7.3×10^{-05}) and clathrin-mediated endocytosis (Reactome; FDR = 8.8×10^{-03}) (Supplementary Table 22).

When compared with pathways up-/downregulated in APOE ϵ 4 carriers, downregulation of mitochondrial metabolism (Reactome; FDR = 3.6×10^{-07}) overlaps with BHBA, while downregulation of neurexin & neuroligins/synapse formation (Reactome; FDR = 2.4×10^{-09}) and clathrin-mediated endocytosis (Reactome; FDR = 2.3×10^{-04}) overlaps with that of valine.

Proteins involved in the transport of BHBA and BCAAs across the blood brain barrier (BBB) and mitochondria

The inverse associations of BHBA and BCAAs in plasma and brain may be explained by a dysfunction of the BBB. Therefore, we investigated BBB and mitochondrial transporters for these metabolites in relation to AD, MCI, and AD pathology in brain in ROSMAP (Supplementary Table 23). The neuronal transporter of BHBA MCT2 (SLC16A7) was marginally downregulated in the brain in those with mild cognitive impairment (beta = -1.63, p -value = 0.04). A similar trend was observed for AD and AD pathology but was not significant. However, the BBB transporter

of BHBA MCT1 (SLC16A1) was not differentially regulated in those with MCI, AD or AD pathology. The BBB BCAA transporter LAT1 (SLC7A5) was significantly downregulated in the brain in AD (beta = -3.61, p -value = 3.5×10^{-03}) and AD pathology including amyloid (CERAD; p -value = 5.01×10^{-05}) and tau (Braak; p -value = 1.38×10^{-05}). For APOE ϵ 4, we found that SLC4A10 was significantly downregulated. SLC4A10 is a sodium/bicarbonate cotransporter which plays an important role in regulating intracellular pH [30], and may contribute to the secretion of cerebrospinal fluid (by similarity). In genome wide association studies, the gene encoding the solute carrier is implicated in cortical thickness, hippocampal and total brain volume, and cognitive function. Further, several mitochondrial transporters (SLC25A6, SLC25A11, SLC25A27 and SLC25A46) were marginally downregulated in APOE ϵ 4 carriers and in AD pathology (Supplementary Table 23) while BCAA transporter (SLC6A15) and mitochondrial glutamate transporter (SLC25A13) were upregulated.

DISCUSSION

Combining data from 274,259 individuals from the UK Biobank and the results of Mendelian randomisation, we find that early pathology underlying AD leads to an increase in plasma levels of BHBA and decrease in the levels of BCAAs (valine, leucine and isoleucine). High plasma BHBA was significantly associated with lower fluid intelligence and higher reaction time in non-demented individuals and an increased risk of future AD and dementia. Increased concentration of plasma BHBA in APOE ϵ 4⁺ is seen decades before the onset of dementia and remains high throughout the studied age range of 37–73 years independent of other comorbidities. We further find that plasma BHBA levels associate with NEFL, a marker for neurodegeneration, and GFAP, a marker for brain inflammation. These observations suggest that high plasma BHBA could be an early marker of ongoing subclinical AD pathology, which is paralleled by low levels in the brain. The BCAAs were found to be decreased in persons at increased risk of AD and dementia and associate with hippocampal volume, fluid intelligence reaction time and fractional anisotropy. MR suggests that plasma BCAAs decrease as a consequence of the subclinical disease process. However, decline in BCAA concentration in the plasma of non-demented APOE ϵ 44 carriers appears to start after the age of 60, suggesting it to be a late(r) life consequence. In the brain the association patterns are reverse, i.e., concentrations of BHBA are decreased and those of BCAAs are increased along with AD pathology. Proteomics analysis in plasma suggests that downregulated proteins in APOE ϵ 4⁺ localized in the lysosome play a key role in the upregulation of BHBA while downregulated proteins in APOE ϵ 4⁺ that are enriched in IGF transport and uptake and immune system pathways overlap with the differential regulation of both BHBA and BCAAs in plasma. In brain, we find strong evidence for downregulation of proteins involved in the TCA cycle, neurexin & neuroligins/synapse formation, and clathrin-mediated endocytosis in APOE ϵ 4⁺, the latter two correspond directly with upregulation of valine in the brain.

BHBA is a ketone body synthesized from fatty acid oxidation in the mitochondria in the hepatocytes [31] and transported to the brain via the BBB transporter MCT1 (SLC16A1) as an energy substrate in the absence of glucose [32]. While astrocytes are also ketogenic, most BHBA in the brain is supplied by the liver [32]. BHBA is considered as a more efficient energy source compared to glucose, yielding more free energy per mole of oxygen to fuel ATP production and fewer by-products of reactive oxygen species [33]. Since glucose metabolism is impaired in AD, ketogenic diets have been shown to improve cognitive symptoms in those with mild cognitive impairment or AD over a short period of time [34]. These benefits, however, are limited to APOE ϵ 4⁺ in both human and animal studies [34]. In APOE ϵ 4⁺ despite rise in the plasma concentration of BHBA after ketogenic diet, no improvements in

cognition have been observed in all intervention studies [34]. In our study, we observed high plasma levels of BHBA in the prospective AD patients, which is consistent with previous studies [5, 6]. We further observed that BHBA levels were higher in *APOE* $\epsilon 4^+$ compared to *APOE* $\epsilon 4^-$ across the age range of 37–73 even in completely healthy individuals, which is consistent with decreased brain glucose metabolism observed in healthy *APOE* $\epsilon 4^+$ individuals aged 20–39 with fluorodeoxyglucose positron emission tomography (FDG-PET) [35]. We also found that the BHBA levels in the brain were low in AD pathology and in *APOE* $\epsilon 4^+$ (albeit not significant). This suggests impaired energy metabolism, in particular glucose metabolism, in *APOE* $\epsilon 4^+$ early on in life, which triggers ketosis in the liver, producing ketone bodies to be used as energy substrates. Under normal hypoglycemic circumstances increased plasma concentration of BHBA increases the expression of MCT1 (SLC16A1) – mono carboxylate transporter of the BBB – leading to a greater influx of the metabolite in the brain [32]. However, in our study, we did not observe increased expression of MCT1 in the brain. Together, these observations suggest that increased plasma concentration of BHBA does not lead to an increase in the brain levels in *APOE* $\epsilon 4^+$ as one would expect under normal hypoglycaemia, suggesting problems in the uptake of BHBA at the BBB through a yet unknown mechanism. This might explain why ketogenic diets were ineffective in improving cognitive symptoms in *APOE* $\epsilon 4^+$. Secondly, we observed that higher plasma levels of BHBA were associated with poorer fluid intelligence and reaction time in non-demented individuals in our study. This finding is in contrast to the earlier reported benefits of ketone bodies on cognitive function [34]. It may be that there are short-term benefits of ketogenesis through improved vascular functioning [36] but in the long-term, the risks outweigh benefits [37, 38]. A question to answer is whether at early age, high plasma levels of BHBA in *APOE* $\epsilon 4^+$ are still associated with high levels in the brain but that with aging there develops a resistance preventing BHBA entry into the brain.

Besides being a secondary energy source, BHBA also acts as a histone deacetylase inhibitor, modulating transcription and translation of proteins involved in various physiological processes [33], including altering the permeabilities of endothelium and epithelium tissues to support pivotal processes and reducing the activities of some high energy-consuming cells [33]. Ketogenic diet has been associated with reduced gut microbial diversity and composition, and an increase in the abundance of pro-inflammatory bacteria [39], dysregulation of mitochondrial function, cardiac fibrosis and inflammation [40, 41]. Because of these conflicting reports, ketone bodies have been termed as a “double-edged sword” [33, 42]. Our own in-depth analysis of the proteomic signatures of BHBA in plasma showed upregulation of several molecular and biological processes including immune system, hemostasis and lysosome, and downregulation of glycosaminoglycan binding, nitrogen metabolism, vitamin digestion and absorption and neurogenesis. Since an increase in the plasma concentration of ketone bodies signals energy deficiency in the body, it is intuitive to think that their elevated concentration will lead the body to prioritise some vital functions at the cost of others for energy conservation [33], which is acceptable for a short period but undesirable in the long run as observed in *APOE* $\epsilon 4^+$. A recent study in mice shows that ketogenic diet induces cellular senescence in multiple organs by inducing p53 signalling through adenosine monophosphate-activated protein kinase and increasing p21 [43]. Given these observations, we hypothesise that elevated levels of BHBA in plasma are an early consequence of the disease process in AD modulated by *APOE* $\epsilon 4$, which might contribute to exacerbation of disease symptoms over time.

Reduced levels of BCAAs in the blood of AD patients are long recognised [3, 44–48]. Nevertheless, an interesting novel finding of this study is the distribution of BCAA concentrations in the periphery across the age range. It shows a very different pattern

compared to ketone bodies: the levels of valine increased with age up to 58 years. After the age of 60, BCAA levels decline in all *APOE* genotype carriers but the decline in *APOE* $\epsilon 44$ is steeper and significant. The negative association of BCAAs in the periphery and dementia is independent from the effect of cardiometabolic disorders, as diabetes, cardiovascular diseases and obesity, which are associated with higher levels of valine in the periphery [49–53]. The decrease of BCAA levels after the age of 60 may be related to weight loss observed for patients with AD before diagnosis of disease [54]. When glucose cannot be used as an efficient energy source in the brain anymore, fatty acids derived from stored adipose tissue are the first alternative energy sources [12, 55], thus reducing weight. If fatty acids are no longer available, amino acids derived from muscle tissue may be used for energy production [56]. On the other hand, we identified increased levels of BCAAs in the brain of individuals with AD, which is in the opposite direction of their association in the periphery. This may be explained by the increased requirement of BCAAs in the brain [57]. Due to failing glucose metabolism, besides ketone bodies, more valine in the periphery must be transported to the brain to meet the energy requirements of the brain. Compared to ketone bodies, BCAAs, especially valine, readily cross the BBB via the LAT1 (SLC7A5) transporter in exchange for glutamine [48]. LAT1 expression is concentration-dependent and increases with rising plasma concentrations of BCAAs [48]. We found that LAT1 was down-regulated in the brain in AD and AD pathology. Given low concentration of BCAAs in the plasma of future AD patients, their accumulation in the brain may be reflective of their defective metabolism in the brain. BCAAs catabolism is dependent on mitochondrial enzymes [48]. Our brain proteomic signatures of *APOE* $\epsilon 4$ revealed that the entire mitochondrial machinery was downregulated in *APOE* $\epsilon 4^+$ and with AD pathology, including TCA cycle enzymes as well as the mitochondrial transporters. To be used as energy substrates by mitochondria, BCAAs (valine in particular) rely on gluconeogenesis [58]. It is therefore intuitive to think that the accumulation of BCAAs in the brain points towards their defective catabolism.

Of note is that of the 85 metabolites associated with dementia, we could only link four, BHBA and the three BCAAs, valine, leucine and isoleucine to AD using Mendelian Randomisation based on our knowledge of the genetics of AD. This does not imply that the other metabolites, in particular the lipids are not biologically relevant. For instance, downregulation of BHBA levels in the brain is associated with an abundance of proteins implicated in cholesterol metabolism. When comparing the metabolomic signatures of dementia with that of its early endophenotypes, results were overall consistent for VLDL subfractions, triglycerides, BCAAs and fatty acids. The study does suggest that bioenergetic pathways and perhaps metabolism in general is completely disturbed in dementia patients.

Despite the large sample size of the study, we still did not have sufficient power to detect associations with VAD as the number of cases was low in the UK Biobank. Secondly, the age range in the UK Biobank is 37–73 years at recruitment, which limited our ability to study *APOE* related changes in the metabolites in younger people. From a clinical perspective, it would be interesting to find out the exact age at which this metabolic shift, i.e., from glucose to ketones happens in *APOE* $\epsilon 4$ carriers as our data shows that it happens before the age of 40. In the ROSMAP dataset, there were a very few *APOE* $\epsilon 44$ carriers, which resulted in a very low statistical power to detect associations particularly in identifying metabolomic and proteomic signatures of *APOE*. Further, ROSMAP data consists of very old participants (age >70 years), consequently it is not possible to determine early life changes in the brain metabolomics and proteomics in *APOE* $\epsilon 4^+$. This also made it difficult to make a comparison with UK Biobank and might explain the opposite effects of BHBA and BCAAs observed in plasma and brain. Besides the age difference, the technical differences, i.e., in

metabolomics assessment, adjustment for confounders, the inherent difference in tissues (as gene expressions are tissue specific) and the sample size might explain the plasma-brain discrepancies observed in our study. Fourth, the differences in proteomics measurements in plasma and brain, especially in the coverage of proteins made it difficult to compare the identified proteomic pathways. Finally, we have based our conclusions on cross-sectional data, longitudinal assessment of metabolites in plasma will provide a more accurate picture of how these metabolites behave over time in cases and controls.

In conclusion, we find that the concentrations of BHBA and BCAAs in plasma and brain are differentially regulated in AD patients and modulated by age and *APOE* ϵ 4. High concentration of plasma BHBA in blood may be a potential early marker of AD to be studied further and our findings raises a question about the effectiveness of interventions on BHBA in *APOE* ϵ 4 carriers, which may have adverse effects. The low levels of valine in blood begs for further research on the interplay between *APOE* ϵ 4, sarcopenia, aging and energy metabolism including mitochondrial function and the TCA cycle, particularly in the early phase of AD. A clinical question to be answered is to what extent the lack of energy interferes with the disease pathology and with the outcome of trials. The proteomics signatures of *APOE*, BHBA and BCAAs suggest downregulation of mitochondrial metabolism but also involves the lysosome and immune system.

ETHICS APPROVAL AND CONSENT TO PARTICIPATE

UK Biobank

All participants provided electronically signed informed consent. UK Biobank has approval from the North West Multi-centre Research Ethics Committee, the Patient Information Advisory Group, and the Community Health Index Advisory Group.

ROSMAP

All procedures and research protocols were approved by the corresponding ethical committees of collaborator's institutions as well as the Institutional Review Board (IRB) of Columbia University Medical Center (protocol AAAR4962). More details can also be found in the website of Rush Alzheimer's Disease Center (RADC; <https://www.radc.rush.edu/>). All participants provided written informed consent for their involvement and use of their data and tissue for research.

DATA AVAILABILITY

UK Biobank data are available through a procedure described at <http://www.ukbiobank.ac.uk/using-the-resource/>. Data from ROSMAP are available through the Rush AD Center Resource Sharing Hub (<https://www.radc.rush.edu/>). All the summary statistics are available in the supplementary tables. Metabolomics data and pre-processed data are accessible through the AD Knowledge Portal (<https://adknowledgeportal.synapse.org/>).

REFERENCES

- Livingston G, Huntley J, Sommerlad A, Ames D, Ballard C, Banerjee S, et al. Dementia prevention, intervention, and care: 2020 report of the Lancet Commission. *Lancet*. 2020;396:413–46.
- Kao Y-C, Ho P-C, Tu Y-K, Jou IM, Tsai K-J. Lipids and Alzheimer's disease. *Int J Mol Sci*. 2020;21:E1505.
- Tynkynen J, Chouraki V, van der Lee SJ, Hernesniemi J, Yang Q, Li S, et al. Association of branched-chain amino acids and other circulating metabolites with risk of incident dementia and Alzheimer's disease: a prospective study in eight cohorts. *Alzheimers Dement*. 2018;14:723–33.
- van der Lee SJ, Teunissen CE, Pool R, Shipley MJ, Teumer A, Chouraki V, et al. Circulating metabolites and general cognitive ability and dementia: evidence from 11 cohort studies. *Alzheimers Dement*. 2018;14:707–22.
- Buergel T, Steinfeldt J, Ruyoga G, Pietzner M, Bizzarri D, Vojinovic D, et al. Metabolomic profiles predict individual multidisease outcomes. *Nat Med*. 2022;28:2309–20.

- Zhang X, Hu W, Wang Y, Wang W, Liao H, Zhang X, et al. Plasma metabolomic profiles of dementia: a prospective study of 110,655 participants in the UK Biobank. *BMC Med*. 2022;20:252.
- Emmerzaal TL, Kiliaan AJ, Gustafson DR. 2003–2013: a decade of body mass index, Alzheimer's disease, and dementia. *J Alzheimers Dis*. 2015;43:739–55.
- Gustafson DR, Backman K, Joas E, Waern M, Ostling S, Guo X, et al. 37 years of body mass index and dementia: observations from the prospective population study of women in Gothenburg, Sweden. *J Alzheimers Dis*. 2012;28:163–71.
- van der Lee SJ, Wolters FJ, Ikram MK, Hofman A, Ikram MA, Amin N, et al. The effect of *APOE* and other common genetic variants on the onset of Alzheimer's disease and dementia: a community-based cohort study. *Lancet Neurol*. 2018;17:434–44.
- Shinohara M, Kanekiyo T, Tachibana M, Kurti A, Shinohara M, Fu Y, et al. *APOE2* is associated with longevity independent of Alzheimer's disease. *Elife*. 2020;9:e62199.
- Abondio P, Sazzini M, Garagnani P, Boattini A, Monti D, Franceschi C, et al. The genetic variability of *APOE* in different human populations and its implications for longevity. *Genes (Basel)*. 2019;10:222.
- Area-Gomez E, Larrea D, Pera M, Agrawal RR, Guilfoyle DN, Pirhaji L, et al. *APOE4* is associated with differential regional vulnerability to bioenergetic deficits in aged *APOE* mice. *Sci Rep*. 2020;10:4277.
- Sudlow C, Gallacher J, Allen N, Beral V, Burton P, Danesh J, et al. UK biobank: an open access resource for identifying the causes of a wide range of complex diseases of middle and old age. *PLoS Med*. 2015;12:e1001779.
- Bennett DA, Buchman AS, Boyle PA, Barnes LL, Wilson RS, Schneider JA. Religious Orders Study and rush memory and aging project. *J Alzheimers Dis*. 2018;64:S161–S89.
- Vonsattel JPG, Amaya MDP, Cortes EP, Mancevska K, Keller CE. Twenty-first century brain banking: practical prerequisites and lessons from the past: the experience of New York Brain Bank, Taub Institute, Columbia University. *Cell Tissue Bank*. 2008;9:247–58.
- Johnson ECB, Dammer EB, Duong DM, Ping L, Zhou M, Yin L, et al. Large-scale proteomic analysis of Alzheimer's disease brain and cerebrospinal fluid reveals early changes in energy metabolism associated with microglia and astrocyte activation. *Nature Medicine*. 2020;26:769–80.
- Davies G, Lam M, Harris SE, Trampush JW, Luciano M, Hill WD, et al. Study of 300,486 individuals identifies 148 independent genetic loci influencing general cognitive function. *Nat Commun*. 2018;9:2098.
- Newell KL, Hyman BT, Growdon JH, Hedley-Whyte ET. Application of the National Institute on Aging (NIA)-Reagan Institute criteria for the neuropathological diagnosis of Alzheimer disease. *J Neuropathol Exp Neurol*. 1999;58:1147–55.
- Braak H, Braak E. Neuropathological staging of Alzheimer-related changes. *Acta Neuropathol*. 1991;82:239–59.
- Wu Y, Byrne EM, Zheng Z, Kemper KE, Yengo L, Mallett AJ, et al. Genome-wide association study of medication-use and associated disease in the UK Biobank. *Nat Commun*. 2019;10:1891.
- Liu J, Lahousse L, Nivard MG, Bot M, Chen L, van Klinken JB, et al. Integration of epidemiologic, pharmacologic, genetic and gut microbiome data in a drug-metabolite atlas. *Nat Med*. 2020;26:110–7.
- Bycroft C, Freeman C, Petkova D, Band G, Elliott LT, Sharp K, et al. The UK Biobank resource with deep phenotyping and genomic data. *Nature*. 2018;562:203–9.
- Julkunen H, Cichońska A, Slagboom PE, Würtz P, Nightingale Health UKBI. Metabolic biomarker profiling for identification of susceptibility to severe pneumonia and COVID-19 in the general population. *Elife*. 2021;10:e63033.
- Sun BB, Chiou J, Traylor M, Benner C, Hsu YH, Richardson TG, et al. Plasma proteomic associations with genetics and health in the UK Biobank. *Nature*. 2023;622:329–38.
- Batra R, Arnold M, Wörheide MA, Allen M, Wang X, Blach C, et al. The landscape of metabolic brain alterations in Alzheimer's disease. *Alzheimers Dement*. 2023;19:980–98. 2022
- Novotny BC, Fernandez MV, Wang C, Budde JP, Bergmann K, Eteleeb AM, et al. Metabolomic and lipidomic signatures in autosomal dominant and late-onset Alzheimer's disease brains. *Alzheimers Dement*. 2023;19:1785–99.
- Wingo AP, Fan W, Duong DM, Gerasimov ES, Dammer EB, Liu Y, et al. Shared proteomic effects of cerebral atherosclerosis and Alzheimer's disease on the human brain. *Nat Neurosci*. 2020;23:696–700.
- Kunkle BW, Grenier-Boley B, Sims R, Bis JC, Damotte V, Naj AC, et al. Genetic meta-analysis of diagnosed Alzheimer's disease identifies new risk loci and implicates *Abeta*, tau, immunity and lipid processing. *Nat Genet*. 2019;51:414–30.
- Richardson TG, Leyden GM, Wang Q, Bell JA, Elsworth B, Davey Smith G, et al. Characterising metabolomic signatures of lipid-modifying therapies through drug target mendelian randomisation. *PLoS Biol*. 2022;20:e3001547.
- Parker MD, Musa-Aziz R, Rojas JD, Choi I, Daly CM, Boron WF. Characterization of human SLC4A10 as an electroneutral Na/HCO₃ cotransporter (NBCn2) with Cl⁻-self-exchange activity. *J Biol Chem*. 2008;283:12777–88.

31. Dedkova EN, Blatter LA. Role of beta-hydroxybutyrate, its polymer poly-beta-hydroxybutyrate and inorganic polyphosphate in mammalian health and disease. *Front Physiol.* 2014;5:260.
32. Achanta LB, Rae CD. β -hydroxybutyrate in the brain: one molecule, multiple mechanisms. *Neurochem Res.* 2017;42:35–49.
33. Qi J, Gan L, Fang J, Zhang J, Yu X, Guo H, et al. Beta-hydroxybutyrate: a dual function molecular and immunological barrier function regulator. *Front Immunol.* 2022;13:805881.
34. Altayyar M, Nasser JA, Thomopoulos D, Bruneau M Jr. The implication of physiological ketosis on the cognitive brain: a narrative review. *Nutrients.* 2022;14:513.
35. Reiman EM, Chen K, Alexander GE, Caselli RJ, Bandy D, Osborne D, et al. Functional brain abnormalities in young adults at genetic risk for late-onset Alzheimer's dementia. *Proc Natl Acad Sci USA.* 2004;101:284–9.
36. Dynka D, Kowalczek K, Charuta A, Paziowska A. The ketogenic diet and cardiovascular diseases. *Nutrients.* 2023;15:3368.
37. Crosby L, Davis B, Joshi S, Jardine M, Paul J, Neola M, et al. Ketogenic diets and chronic disease: weighing the benefits against the risks. *Front Nutr.* 2021;8:702802.
38. Batch JT, Lamsal SP, Adkins M, Sultan S, Ramirez MN. Advantages and disadvantages of the ketogenic diet: a review article. *Cureus.* 2020;12:e9639.
39. Paoli A, Mancin L, Bianco A, Thomas E, Mota JF, Piccini F. Ketogenic diet and microbiota: friends or enemies? *Genes (Basel).* 2019;10:534.
40. Xu S, Tao H, Cao W, Cao L, Lin Y, Zhao SM, et al. Ketogenic diets inhibit mitochondrial biogenesis and induce cardiac fibrosis. *Signal Transduct Target Ther.* 2021;6:54.
41. Tao J, Chen H, Wang YJ, Qiu JX, Meng QQ, Zou RJ, et al. Ketogenic diet suppressed T-regulatory cells and promoted cardiac fibrosis via reducing mitochondria-associated membranes and inhibiting mitochondrial function. *Oxid Med Cell Longev.* 2021;2021:5512322.
42. Tomita I, Tsuruta H, Yasuda-Yamahara M, Yamahara K, Kuwagata S, Tanaka-Sasaki Y, et al. Ketone bodies: a double-edged sword for mammalian life span. *Aging Cell.* 2023;22:e13833.
43. Wei SJ, Schell JR, Chocron ES, Varmazyad M, Xu G, Chen WH, et al. Ketogenic diet induces p53-dependent cellular senescence in multiple organs. *Sci Adv.* 2024;10:eado1463.
44. Murrell JR, Hake AM, Quaid KA, Farlow MR, Ghetti B. Early-onset Alzheimer disease caused by a new mutation (V717L) in the amyloid precursor protein gene. *Arch Neurol.* 2000;57:885–7.
45. Xiong YL, Theriault J, Ren SJ, Jing XJ, Zhang H. Alzheimer's Disease Neuroimaging I. The associations of serum valine with mild cognitive impairment and Alzheimer's disease. *Aging Clin Exp Res.* 2022;34:1807–17.
46. Arnold M, Nho K, Kueider-Paisley A, Massaro T, Huynh K, Brauner B, et al. Sex and APOE ϵ 4 genotype modify the Alzheimer's disease serum metabolome. *Nat Commun.* 2020;11:1148.
47. Nho K, Kueider-Paisley A, Arnold M, MahmoudianDehkordi S, Risacher SL, Louie G, et al. Serum metabolites associated with brain amyloid beta deposition, cognition and dementia progression. *Brain Communications.* 2021;3:fcab139.
48. Polis B, Samson A. Role of the metabolism of branched-chain amino acids in the development of Alzheimer's disease and other metabolic disorders. *Neural Regeneration Research.* 2020;15:1460–70.
49. Wang TJ, Larson MG, Vasan RS, Cheng S, Rhee EP, McCabe E, et al. Metabolite profiles and the risk of developing diabetes. *Nature Medicine.* 2011;17:448–53.
50. Bloomgarden Z. Diabetes and branched-chain amino acids: what is the link? *J Diabetes.* 2018;10:350–2.
51. Flores-Guerrero JL, Groothof D, Connelly MA, Otvos JD, Bakker SJL, Dullaart RPF. Concentration of branched-chain amino acids is a strong risk marker for incident hypertension. *Hypertension.* 2019;74:1428–35.
52. Roberts LD, Koulman A, Griffin JL. Towards metabolic biomarkers of insulin resistance and type 2 diabetes: progress from the metabolome. *Lancet Diabetes Endocrinol.* 2014;2:65–75.
53. Ruiz-Canela M, Toledo E, Clisb CB, Hruby A, Liang L, Salas-Salvadó J, et al. Plasma branched-chain amino acids and incident cardiovascular disease in the PRE-DIMED trial. *Clin Chem.* 2016;62:582–92.
54. Floud S, Simpson RF, Balkwill A, Brown A, Goodill A, Gallacher J, et al. Body mass index, diet, physical inactivity, and the incidence of dementia in 1 million UK women. *Neurology.* 2020;94:e123–e32.
55. Kuehn BM. In Alzheimer research, glucose metabolism moves to center stage. *JAMA.* 2020;323:297–9.
56. Blaxter KL. Energy metabolism in animals and man / Kenneth Blaxter, Kt. Cambridge [England]: Cambridge University Press; 1989.
57. Salcedo C, Andersen JV, Vinten KT, Pinborg LH, Waagepetersen HS, Freude KK, et al. Functional metabolic mapping reveals highly active branched-chain amino acid metabolism in human astrocytes, which is impaired in iPSC-derived astrocytes in Alzheimer's disease. *Front Aging Neurosci.* 2021;13:736580.
58. Neinast M, Murashige D, Arany Z. Branched chain amino acids. *Annu Rev Physiol.* 2019;81:139–64.

ACKNOWLEDGEMENTS

We thank contributors who collected samples used in this study and patients and their families, whose help and participation made this work possible. This research has been conducted using the UK Biobank Resource under application numbers 30418 and 61054. The Nightingale datasets have been generated at Nightingale Health.

AUTHOR CONTRIBUTIONS

NA, JL, RKD and CMvD designed the study. NA and JL performed the statistical analysis. NA, JL, RKD and CMvD drafted the manuscript. WS, MA, RB, BB, YJC, MF, JK, DN, KN, JPK, LS, LMW, YY, ANH and GK contributed to the interpretation of the findings, writing and critically reviewing the manuscript.

FUNDING

Metabolomics data as well as data preprocessing, analysis, and interpretation is provided by the Alzheimer's Disease Metabolomics Consortium (ADMC) and funded wholly or in part by the following grants and supplements thereto: NIA R01AG046171, RF1AG051550, RF1AG057452, R01AG059093, RF1AG058942, U01AG061359, U19AG063744 and FNIH: #DAOU16AMPA awarded to Dr. Kaddurah-Daouk at Duke University in partnership with a large number of academic institutions. A complete listing of ADMC investigators can be found at: <https://sites.duke.edu/adnimetab/team/>. Metabolomics data and pre-processed data are accessible through the AD Knowledge Portal (<https://adknowledgeportal.synapse.org/>). The AD Knowledge Portal is the distribution site for data, analysis results, analytical methodology and research tools generated by the AMP-AD Target Discovery and Preclinical Validation Consortium and multiple Consortia and research programs supported by the National Institute on Aging. The computational aspects of this research were supported by the Wellcome Trust Core Award Grant Number 203141/Z/16/Z and the Oxford NIHR BRC. The views expressed are those of the author(s) and not necessarily those of the NHS, the NIHR or the Department of Health. ROSMAP data were provided by the Rush Alzheimer's Disease Center, Rush University Medical Center, Chicago. Data collection was supported through funding by NIA grants P30AG10161 (ROS), R01AG15819 (ROSMAP; genomics and RNAseq), R01AG17917 (MAP), R01AG30146, R01AG36042 (5hC methylation, ATACseq), RC2AG036547 (H3K9Ac), R01AG36836 (RNAseq), R01AG48015 (monocyte RNAseq), RF1AG57473 (single nucleus RNAseq), U01AG32984 (genomic and whole exome sequencing), U01AG46152 (ROSMAP AMP-AD, targeted proteomics), U01AG46161 (TMT proteomics), U01AG61356 (whole genome sequencing, targeted proteomics, ROSMAP AMP-AD), the Illinois Department of Public Health (ROSMAP), and the Translational Genomics Research Institute (genomic). Study data were provided through NIA grant 3R01AG046171-02S2 awarded to Rima Kaddurah-Daouk at Duke University, based on specimens provided by the Rush Alzheimer's Disease Center, Rush University Medical Center, Chicago. We thank the participants of ROS and MAP for their essential contributions to these projects. Jan Krumsiek and Richa Batra are supported by the National Institute of Aging of the National Institutes of Health under awards 1U19AG063744 and R01AG069901-01. Richa Batra is also supported by Alzheimer's association award AARFD-22-974775. K.N. receives support from multiple NIH grants (P30 AG010133, P30 AG072976, R01 AG081951, R01 LM012535, U01 AG072177, R01AG081322, and U19 AG074879). Najaf Amin is funded by National Institute on Aging (NIH) and Oxford-GSK Institute of Molecular and Computational Medicine (IMCM). Cornelia M van Duijn is supported by the US National Institute on Aging (NIH), NovoNordisk, the Oxford-GSK Institute of Molecular and Computational Medicine (IMCM), Centre of Artificial Intelligence for Precision Medicines (CAIPM) of the University of Oxford and King Abdul Aziz University, Alzheimer Research UK (ARUK), UK National Institute for Health and Care Research (NIHR) Oxford Research Center (BRC), ZonMW (Delta Dementie) and Alzheimer Nederland. Dr. Saykin receives support from multiple NIH grants (P30 AG010133, P30 AG072976, R01 AG019771, R01 AG057739, U19 AG024904, R01 LM013463, R01 AG068193, R01 AG092591, T32 AG071444, U01 AG068057, U01 AG072177, U19 AG074879, as well as U24 AG074855).

COMPETING INTERESTS

Dr. Kaddurah-Daouk is an inventor on a series of patents on use of metabolomics for the diagnosis and treatment of CNS diseases and holds equity in Metabolon Inc., Chymia LLC and PsyProtix. Dr. Arnold is a co-inventor on patents on applications of metabolomics in diseases of the central nervous system and holds equity in Chymia LLC and IP in PsyProtix and Atai that are exploring the potential for therapeutic applications targeting mitochondrial metabolism in treatment-resistant depression. Jan Krumsiek holds equity in iollo, Chymia LLC and IP in PsyProtix. Dr. Saykin has

received in-kind support from Avid Radiopharmaceuticals, a subsidiary of Eli Lilly (PET tracer precursor) and Gates Ventures, LLC and Sanofi (Proteomics panel assays on IADRC and KBASE participants as part of the Global Neurodegeneration Proteomics Consortium) and gift funds (GV) supporting technical contributions to the GRIP platform. and he has participated in Scientific Advisory Boards (Bayer Oncology, Eisai, Novo Nordisk, and Siemens Medical Solutions USA, Inc) and an Observational Study Monitoring Board (MESA, NIH NHLBI), as well as External Advisory Committees for multiple NIA grants. He also serves as Editor-in-Chief of Brain Imaging and Behavior, a Springer-Nature Journal. Najaf Amin and Cornelia M. van Duijn are funded by Oxford-GSK Institute of Molecular and Computational Medicine (IMCM). Cornelia M van Duijn is currently the Research Director Brain Health of the Health Data Research UK (HDR UK) and the UK Dementia Research Institute (UK DRI), working in partnership with Dementias Platform UK (DPUK). All other authors declare no conflicts of interest.

ADDITIONAL INFORMATION

Supplementary information The online version contains supplementary material available at <https://doi.org/10.1038/s41398-025-03625-8>.

Correspondence and requests for materials should be addressed to Rima Kaddurah-Daouk or Cornelia M. van Duijn.

Reprints and permission information is available at <http://www.nature.com/reprints>

Publisher's note Springer Nature remains neutral with regard to jurisdictional claims in published maps and institutional affiliations.



Open Access This article is licensed under a Creative Commons Attribution-NonCommercial-NoDerivatives 4.0 International License, which permits any non-commercial use, sharing, distribution and reproduction in any medium or format, as long as you give appropriate credit to the original author(s) and the source, provide a link to the Creative Commons licence, and indicate if you modified the licensed material. You do not have permission under this licence to share adapted material derived from this article or parts of it. The images or other third party material in this article are included in the article's Creative Commons licence, unless indicated otherwise in a credit line to the material. If material is not included in the article's Creative Commons licence and your intended use is not permitted by statutory regulation or exceeds the permitted use, you will need to obtain permission directly from the copyright holder. To view a copy of this licence, visit <http://creativecommons.org/licenses/by-nc-nd/4.0/>.

© The Author(s) 2025